

# Universal spectral properties of spatially periodic quantum systems with chaotic classical dynamics

T. Dittrich<sup>1</sup>, B. Mehlig<sup>1</sup>, H. Schanz<sup>1</sup> and U. Smilansky<sup>2</sup>

<sup>1</sup> *Max-Planck-Institut für Physik komplexer Systeme, Bayreuther Str. 40, Haus 16  
01187 Dresden, Germany*

<sup>2</sup> *Department of Physics of Complex Systems, The Weizmann Institute of Science  
Rehovot 76100, Israel*

(November 12, 2018)

## Abstract

We consider a quasi one-dimensional chain of  $N$  chaotic scattering elements with periodic boundary conditions. The classical dynamics of this system is dominated by diffusion. The quantum theory, on the other hand, depends crucially on whether the chain is disordered or invariant under lattice translations. In the disordered case, the spectrum is dominated by Anderson localization whereas in the periodic case, the spectrum is arranged in bands. We investigate the special features in the spectral statistics for a periodic chain. For finite  $N$ , we define spectral form factors involving correlations both for identical and non-identical Bloch numbers. The short-time regime is treated within the semiclassical approximation, where the spectral form factor can be expressed in terms of a coarse-grained classical propagator which obeys a diffusion equation with periodic boundary conditions. In the long-time regime, the form factor decays algebraically towards an asymptotic constant. In the limit  $N \rightarrow \infty$ , we derive a universal scaling function for the form factor. The theory is supported by numerical results for quasi one-dimensional periodic chains of coupled Sinai billiards.

05.45.+b,03.65.Sq

## I. INTRODUCTION

The goal of quantum chaology is to identify universal features which prevail in systems whose classical dynamics is chaotic, and to relate the quantum observables to their classical counterparts. Spectral statistics is one of the topics where this approach has met with success, and the connection between the spectral form factor (the Fourier transform of the two-point correlation function) and the classical probability to stay, is a very fruitful junction of mesoscopic physics and quantum chaos [1–6]. In the present article we develop the corresponding theory for extended, quasi one-dimensional systems.

We consider composite systems consisting of  $N$  chaotic unit cells of length  $a$  with periodic boundary conditions. The example we have in mind is a chain of interconnected chaotic billiards, as shown in Fig. 1. In practice one can realize such systems by constructing a mesoscopic ring with a circumference  $L = Na$  which is smaller than the dephasing mean free path, but much larger than the elastic mean free path. The particle moves as a random walker between the unit cells, which results on average in a diffusive evolution. It is important to note from the outset that the diffusive nature of the classical evolution is completely indifferent to the translational symmetry of the ring — whether it is periodic or disordered. In contrast, quantum mechanics depends crucially on this feature: disordered rings are affected by Anderson localization and in the limit  $N \rightarrow \infty$  the spectrum remains discrete with a Poissonian spectral statistics [3]. Chains which are invariant under discrete lattice translations develop continuous band spectra in the same limit. Can one account for these two different quantum situations within a theory that relies on the classical diffusive evolution which in itself is indifferent to the symmetry? The present work provides an affirmative answer to this question. We study in particular the spectral form factor for the periodic case, and show that in the limit  $N \rightarrow \infty$ , it approaches a limit distribution which expresses the effect of the levels clustering into bands.

Let us consider the two scenarios in some more detail: In the *disordered* case, once the overall length  $L = Na$  is sufficiently larger than the Anderson localization length  $\xi$ , one can consider the system qualitatively as a union of  $L/\xi$  uncoupled systems. Within this picture, the spectrum is a superposition of uncorrelated spectra, resulting in a spectral form factor  $K_N(\tau) \simeq K_1(\tau L/\xi)$ , where the suffix 1 denotes the spectral form factor for the unit cell, as opposed to the form factor  $K_N(\tau)$  for the composite system.

In the *periodic* case, the symmetry with respect to discrete lattice translations implies the existence of discretized energy bands. According to Bloch's theorem, the energies are labeled by a quasi-momentum (Bloch number)  $q$  which takes discrete values for a finite chain. Energy levels with different Bloch numbers are correlated over some range in  $q$ . Hence, on the time scale corresponding to an energy scale of the order of the inter-band spacing, the spectrum looks as if it were degenerate with a multiplicity  $\sim N$ . This corresponds to a peak  $\sim N$  in the form factor  $K_N(\tau)$  at  $\tau \sim 1/N$ . For larger times, finer structures in the spectrum are resolved, until for very large times ( $\tau \gtrsim 1$ ), the discrete nature of the spectrum is the dominant feature. On this time scale  $K_N(\tau) \simeq 1$  (in the absence of symmetries). As will be shown in this paper, the interpolation between the two time scales is given by a power-law decay  $K_N(\tau) \sim 1/\tau$ .

Since we are dealing here with the periodic case, we make use of the extra parameter which quantum mechanics provides, and consider spectral statistics which test the corre-

lations between spectra of different Bloch numbers. We develop a semiclassical theory for these spectral measures and show that they are intimately connected with the distribution of winding numbers in the symmetry-reduced classical system, which in the present case is the unit cell with periodic boundary conditions. This analysis makes use of the general formalism proposed by Robbins [7], and can be considered as an extension of the previous work on band spectra in chaotic systems [8].

It is important to emphasize that the considerations given above are rather general and do not depend on the details of the actual system. To check the universality of our arguments we have performed a parallel study where the system of interest is not a billiard chain, but an appropriately defined version of the quantum kicked rotor [9]. This work will be reported elsewhere [10]. The results obtained for the two models agree in all details, giving credence to our claim that the spectral statistics for periodic diffusive chains are universal.

The paper is organized as follows. In section II we derive a secular equation for the energy spectrum of the billiard chain. It is based on the scattering approach to quantization [11] and used here to compute the spectrum numerically. The quantities allowing us to study spectral correlations for periodic quantum systems are introduced in section III. Section IV is devoted to the semiclassical theory of the form factor for small times ( $\tau \lesssim 1/N$ ), while in section V we discuss the form factor for intermediate times ( $1/N \lesssim \tau < 1$ ). Finally, in section VI, we summarize our results.

## II. QUANTUM MECHANICS

In the present section we describe the quantization of the system shown in Fig. 1(a). It is composed of  $N$  identical unit cells of length  $a$  which form a quasi one-dimensional chain of total length  $L = Na$ . Each unit cell represents a waveguide of unit width with two half-discs as shown in Fig. 3. The radii are denoted by  $R_-$  and  $R_+$ , respectively. The wave function  $\psi(x, y)$  satisfies the Schrödinger equation

$$-\frac{\hbar^2}{2m}\Delta\psi(x, y) = E\psi(x, y) \quad (1)$$

with Dirichlet boundary conditions on the walls of the waveguide and periodic boundary conditions in  $x$ -direction

$$\psi(x + L, y) = \psi(x, y). \quad (2)$$

Moreover, as shown in Fig. 1(a), the system is invariant under discrete lattice translations  $x \rightarrow x + a$ . In conjunction with (2), the translational symmetry implies the existence of discretized energy bands  $E_\alpha(q)$ . The energies are labeled by a discrete set of Bloch numbers

$$q = \frac{2\pi\nu}{L}, \quad \nu = 0, \dots, N - 1 \quad (3)$$

in the first Brillouin zone, corresponding to the  $N$  irreducible representations of the group of lattice translations. A typical band spectrum  $E_\alpha(q)$  is shown in Fig. 2. The wave functions can be classified according to their Bloch numbers and can be written as

$$\psi_q(x, y) = \exp(iqx) u_q(x, y), \quad (4)$$

where  $u_q(x, y)$  is periodic in  $x$  with period  $a$  (Bloch's theorem). Hence, for every Bloch number  $q$  one has the quantization condition

$$\begin{aligned} -\frac{\hbar^2}{2m}\Delta\psi_q(x, y) &= E(q)\psi_q(x, y), \\ \psi_q(x+a, y) &= \exp(iqa)\psi_q(x, y). \end{aligned} \quad (5)$$

Obviously, the spectrum  $E_\alpha(q)$  has the following symmetries

$$E_\alpha(q + 2\pi/a) = E_\alpha(q), \quad (6)$$

$$E_\alpha(-q) = E_\alpha(q). \quad (7)$$

In what follows we discuss an implementation of the quantization condition (5). Due to the translational invariance, it is sufficient to quantize a single unit cell with periodic boundary conditions including an additional phase  $\exp(iqa)$ , as shown in Fig. 3. In the straight-channel sections of the unit cell, the wave function can be decomposed into normal modes

$$\psi_q(x, y) = \sum_{j=1}^{\infty} \frac{\phi_j(y)}{\sqrt{k_j}} \left( a_{j_s}^{(+)} e^{+isk_j(x-x_s)} + a_{j_s}^{(-)} e^{-isk_j(x-x_s)} \right), \quad (8)$$

where

$$\phi_j(y) = \sqrt{2} \sin(j\pi y), \quad (9)$$

and the index  $s = \mp$  designates the l.h.s. and r.h.s. of the unit cell, respectively. The index  $n$  labels the normal modes, with wave numbers  $k_n$  defined according to

$$k_j = \begin{cases} \sqrt{k^2 - (j\pi)^2} & \text{for open modes } (j \leq \Lambda(E)) \\ i\sqrt{(j\pi)^2 - k^2} & \text{for closed modes } (j > \Lambda(E)), \end{cases} \quad (10)$$

where  $\hbar k = \sqrt{2mE}$ . The number of open modes  $\Lambda(E)$  is given by the integer part of  $k/\pi$ . For an open mode,  $a_{j_s}^{(-)}$  represents the amplitude of the incoming and  $a_{j_s}^{(+)}$  that of the outgoing partial wave. As the semicircular obstacles are approached, the partial waves for  $j > \Lambda(E)$  decrease (increase) exponentially. The coefficients of the partial waves to the left and to the right of the obstacles can be related to each other using Eq. (5). One has  $a_{j,+}^{(\pm)} = e^{iqa} a_{j,-}^{(\mp)}$ , which can be written as a matrix equation

$$\begin{pmatrix} a_{-}^{(-)} \\ a_{+}^{(-)} \end{pmatrix} = \Gamma(q) \begin{pmatrix} a_{-}^{(+)} \\ a_{+}^{(+)} \end{pmatrix} \quad (11)$$

with

$$\Gamma_{j_s, j'_s}(q) = \delta_{j, j'} \delta_{s, -s'} e^{isqa}. \quad (12)$$

We will now express the condition (11) in terms of the generalized scattering matrix  $S(E)$  of the obstacle [11] which provides a convenient starting point for both the numerical implementation and the semiclassical theory. For this purpose, we consider the Green function

in the unit cell which satisfies  $[\Delta + k^2] G(\mathbf{r}, \mathbf{r}') = -\delta(\mathbf{r} - \mathbf{r}')$ , with Dirichlet boundary conditions on the walls of the waveguide and outgoing boundary conditions at the borders of the unit cell. In the straight-channel sections,  $G(\mathbf{r}, \mathbf{r}')$  can be written in the normal-mode decomposition

$$G(x, y; x', y') = \frac{i}{2} \sum_{j, j'} \frac{\phi_j(y)}{\sqrt{k_j}} \frac{\phi_{j'}(y')}{\sqrt{k_{j'}}} \left( \delta_{j, j'} \delta_{s, s'} e^{ik_j|x-x'|} + S_{j_s, j'_s} e^{isk_j(x-x_s) + is'k_{j'}(x'-x_{s'})} \right). \quad (13)$$

The matrix  $S$  depends on the particular geometry and remains to be determined. Using (8), (13) and Green's theorem for the unit cell it is straightforward to show that  $S$  transforms the amplitudes of the incoming partial waves into those of the outgoing ones,

$$\begin{pmatrix} a_-^{(+)} \\ a_+^{(+)} \end{pmatrix} = S \begin{pmatrix} a_-^{(-)} \\ a_+^{(-)} \end{pmatrix}, \quad (14)$$

for any solution of (1). Hence, it can be regarded as a generalized scattering matrix for the obstacle in the waveguide. The usual unitary  $S$ -matrix is obtained by restricting  $n$  and  $n'$  to open modes. We note that  $S$  may be written in block form

$$S = \begin{pmatrix} r & t' \\ t & r' \end{pmatrix}, \quad (15)$$

in terms of the reflection and transmission matrices  $r, r'$  and  $t, t'$ , respectively. The phase shifts are defined as in Ref. [12] such that  $S_{j_s, j'_s} = \delta_{j, j'} \delta_{s, -s'} e^{ik_j a}$  for an empty unit cell of length  $a$ . Using (11) to eliminate the coefficients of the outgoing waves in (14) we find

$$[1 - \Gamma(q) S(E)] \begin{pmatrix} a_-^{(-)} \\ a_+^{(-)} \end{pmatrix} = 0, \quad (16)$$

which can be satisfied by some combination of incoming waves provided that

$$\det[1 - \Gamma(q) S(E)] = 0. \quad (17)$$

This is the secular equation for the spectrum within the scattering approach to quantization [11,13]. Together with the method described in appendix A for the computation of the matrix  $S$ , Eq. (17) can be used to obtain the energy spectrum of the periodic chain of scatterers numerically. For this purpose one restricts  $S$  to a finite matrix. In order to obtain well-converged eigenvalues, at least four closed modes have to be taken into account in the present case.

### III. SPECTRAL CORRELATIONS IN PERIODIC SYSTEMS

In the present section we discuss the spectral properties of quasi one-dimensional periodic systems. A typical spectrum is shown in Fig. 2 (for  $N = 32$ ). The spectral correlations are expressed in terms of the density of states

$$d(E, q) = \sum_{\alpha} \delta(E - E_{\alpha}(q)). \quad (18)$$

It is convenient to decompose the density of states into a mean and an oscillatory part,  $d = \langle d \rangle + \tilde{d}$ . Note that  $\langle d \rangle$  is the mean density of states for a given Bloch number. In other words, it is the mean density of states associated with one unit cell. In order to emphasize this, the mean density will henceforth be denoted as  $\langle d_1 \rangle$ . As usual, we unfold the spectrum [14] in order to obtain a unit total mean density. This is achieved by

$$x_{\alpha}(q) = N \langle d_1 \rangle E_{\alpha}(q), \quad (19)$$

where the energy dependence of the mean density of states has been neglected. Note that the unfolding of the spectrum is done with respect to the area of the entire chain [16] We define the unfolded density of states according to

$$d(x, q) = \sum_{\alpha} \delta(x - x_{\alpha}(q)). \quad (20)$$

The spectral form factor  $K_N(q, q'; \tau)$  is then defined as

$$K_N(q, q'; \tau) = \left\langle \int_{-\infty}^{\infty} d\xi e^{-2\pi i \xi \tau} \tilde{d}(x + \xi/2, q) \tilde{d}(x - \xi/2, q') \right\rangle. \quad (21)$$

Here,  $\tau$  is a rescaled time, related to the physical time  $t$  by  $t = 2\pi\hbar \langle d_1 \rangle N \tau$ . For a finite spectral window the form factor can be expressed as follows [15]

$$K_N(q, q'; \tau) = \frac{N}{\Delta x} \left[ \sum_{\alpha} e^{2\pi i (x - x_{\alpha}(q)) \tau} f(x - x_{\alpha}(q)) - \hat{f}(\tau) \right] \\ \times \left[ \sum_{\alpha'} e^{-2\pi i (x - x_{\alpha'}(q')) \tau} f(x - x_{\alpha'}(q')) - \hat{f}(\tau) \right]. \quad (22)$$

Here,  $f(x)$  is a spectral window function defined according to

$$f(x) = \begin{cases} 1 & \text{for } |x| < \Delta x/2, \\ 0 & \text{otherwise.} \end{cases} \quad (23)$$

$\hat{f}(\tau)$  denotes the Fourier transform of  $f(x)$ . Note that  $f(x)$  is normalized such that its integral equals the number  $\Delta x$  of states contained in the spectral window,

$$\int_{-\infty}^{\infty} dx f(x) = \Delta x.$$

The form factor  $K_N(q, q'; \tau)$  is normalized such that  $K_N(q, q; \tau) \rightarrow 1$  for large  $\tau$ . In fact, for large  $\tau$ , only the diagonal contributions to the double sum in Eq. (22) have to be retained and one has (for  $q$  and  $q'$  not related by the band symmetries discussed in section II)

$$K_N(q, q'; \tau) \simeq \delta_{q, q'} \frac{N}{\Delta x} \sum_{\alpha} f^2(x - x_{\alpha}(q)) \\ \simeq \delta_{q, q'} \frac{1}{\Delta x} \int_{-\infty}^{\infty} dx f^2(x) \\ = \delta_{q, q'}. \quad (24)$$

The fact that the form factor tends to a constant for  $q = q'$  and large  $\tau$  is a consequence of the discrete nature of the spectrum. The corresponding quantum dynamics is governed by quasi-periodic motion on the time scale of the inverse intra-band spacing. According to Eq. (24), correlations between different Bloch numbers decrease rapidly for large  $\tau$ , provided the Bloch numbers are not related by symmetries. An example is given in Fig. 4, where  $K_N(q, q'; \tau)$  is shown for  $q \neq q'$ . As expected, the form factor tends to zero for large  $\tau$ . On the other hand we observe significant cross correlations between different Bloch numbers at intermediate values of  $\tau$ , of the order of  $\tau \simeq 1/N$ . This time scale corresponds to the mean inter-band spacing and the correlations are associated with the existence of energy bands. Before discussing these cross correlations in detail, we consider the spectral correlations at fixed Bloch number  $q$ .

### A. Spectral correlations at fixed Bloch number $q$

In the present subsection we discuss spectral correlations for fixed Bloch number  $q$ . Consider for instance the spectrum shown in Fig. 2. Since the classical dynamics of the unit cell is chaotic, the spectral correlations at fixed  $q$  are expected to be described by random-matrix theory. The quantization condition (5) of section II can be rewritten as follows

$$-\frac{\hbar^2}{2m} \left[ \left( \frac{\partial}{\partial x} + iq \right)^2 + \frac{\partial^2}{\partial y^2} \right] u_q(x, y) \equiv \widehat{H}(q) u_q(x, y) = E(q) u_q(x, y)$$

$$u_q(x + a, y) = u_q(x, y).$$

Obviously, the Bloch number  $q$  can be regarded as reflecting an Aharonov-Bohm flux  $\phi$ , with  $q = 2\pi/a \phi/\phi_0$  and  $\phi_0 = 2\pi\hbar/e$ . For  $q = 0$ , the Hamiltonian  $\widehat{H}(q)$  is invariant with respect to time reversal and the spectral properties are described by the ensemble of Gaussian orthogonal random matrices (GOE). In the case  $q = \pi/a$ ,  $\widehat{H}(q)$  is invariant under the anti-unitary transformation  $\widehat{\theta} = \exp(-2iqx)\widehat{J}$ , where  $\widehat{J}$  is the operator of complex conjugation. For  $q = \pi/a$ , the appropriate ensemble is hence also the orthogonal one (GOE). For  $q = \pi/2a$ , on the other hand, the spectral properties are described by the ensemble of Gaussian unitary random matrices (GUE). As  $q$  changes from zero to  $\pi/2a$ , one expects a crossover from orthogonal to unitary statistics.

Fig. 5 shows the spectral form factor  $K_N(q, q; \tau)$  as a function of  $\tau$  for two different values,  $q = 0$  and  $q = \pi/2a$ , of the Bloch number. The universal results for the orthogonal and unitary ensembles [14] are displayed with solid and dashed lines, respectively. As expected, we observe GOE behaviour for  $q = 0$  and GUE behaviour for  $q = \pi/2a$ . Similarly, the histogram  $P(\Delta)$  of nearest-neighbour spacings exhibits a crossover from GOE to GUE statistics. This is shown in Fig. 6. This crossover occurs on an  $\hbar$ -dependent scale. In the semiclassical limit  $\hbar \rightarrow 0$ , the transition is instantaneous.

### B. Spectral cross correlations

In the present subsection we discuss correlations between different Bloch numbers. These correlations decay rapidly for large  $\tau$ , as shown for instance in Fig. 4. However, it will turn out in the following that spectral cross correlations at intermediate values of  $\tau$  are

of particular importance in extended periodic quantum systems, since they are directly related to the existence of discretized energy bands. In order to analyse correlations between different values of  $q$ , we define

$$S_N(n; \tau) = \frac{1}{N} \sum_{q, q'} e^{in(q-q')a} K_N(q, q'; \tau). \quad (25)$$

Note that  $S_N(0; \tau)$  is just the conventional spectral form factor  $K_N(\tau)$  for the composite system referred to in the introduction. Rewriting  $S_N(n; \tau)$  in terms of a Bloch-number specific density of states

$$d(x, n) = \sum_q e^{inqa} d(x, q), \quad (26)$$

we obtain

$$S_N(n; \tau) = \left\langle \int_{-\infty}^{\infty} d\xi e^{-2\pi i \xi \tau} \tilde{d}(x + \xi/2, n) \tilde{d}(x - \xi/2, n) \right\rangle. \quad (27)$$

In the following, we discuss the long-time asymptote of  $S_N(n; \tau)$ . For a finite spectral window,  $S_N(n; \tau)$  can be expressed in a form similar to Eq. (22) and for  $\tau \gg 1/\Delta x$  one has

$$S_N(n; \tau) \simeq \frac{1}{\Delta x} \left| \sum_q \sum_{\alpha} e^{inqa - 2\pi i x_{\alpha}(q)\tau} f(x - x_{\alpha}(q)) \right|^2. \quad (28)$$

Taking into account the symmetry of the spectrum with respect to  $q \rightarrow 2\pi/a - q$  and in the absence of further symmetries, the phases of the off-diagonal terms in the double sum are random and cancel. Using  $q = 2\pi\nu/L$ , one has

$$\simeq \frac{1}{N} \left[ 2 + 4 \sum_{\nu=1}^{N/2-1} \cos^2 \left( \frac{2\pi\nu n}{N} \right) \right] \frac{1}{\Delta x} \int_{-\infty}^{\infty} dx f^2(x), \quad (29)$$

assuming  $N$  to be an even integer. Using  $\int dx f^2(x) = \Delta x$  (compare Eq. (23)), we obtain

$$= \begin{cases} 2(1 - \frac{1}{N}) & \text{for } n = 0, N/2, \\ 1 - \frac{2}{N} & \text{otherwise.} \end{cases} \quad (30)$$

For large  $N$ ,  $S_N(n; \tau) \rightarrow 2$  for  $n = 0, N/2$ . This is a consequence of the band symmetry (7) discussed in section II.

#### IV. SEMICLASSICAL ANALYSIS

In the following we obtain a semiclassical approximation for  $S_N(n; \tau)$ . This is done in two steps. First, we derive a semiclassical approximation for the density of states for a periodic quantum system. It will be seen below that in the present case it is particularly convenient to start from Eq. (17). As discussed in Ref. [7], the resulting semiclassical expression features the characters  $\chi(n, q) = \exp(inqa)$  of the group of lattice translations. Second, we introduce the diagonal approximation for the form factor. The diagonal approximation is adequate for times smaller than the Heisenberg time of the unit cell, that is for  $t \lesssim t_H = 2\pi\hbar\langle d_1 \rangle$  or equivalently for  $\tau \lesssim 1/N$ . A theory covering the long-time behaviour is worked out in section V.



### A. Semiclassical approximation for the density of states

We now proceed to derive a semiclassical approximation for the energy spectrum. The starting point is Eq. (17), in which  $S(E)$  is restricted to the unitary  $\Lambda \times \Lambda$ -matrix corresponding to the open modes. In this case the spectral density following from (17) may be written as [11]

$$d(E, q) = \sum_{\alpha=1}^{\infty} \delta(E - E_{\alpha}(q)) = \frac{d}{dE} \frac{\Theta(E)}{2\pi} + \frac{d}{dE} \text{Im} \sum_{m=1}^{\infty} \frac{1}{m\pi} \text{Tr} [\Gamma(q)S(E)]^m, \quad (31)$$

where  $\Theta(E) = -i \log \det S(E)$  denotes the total phase of the  $S$ -matrix. Using a theorem by M. G. Krein [17], it is possible to obtain a semiclassical approximation for  $\Theta$  which contains a smooth part given by the generalized Weyl law [18] for the unit cell and an oscillating part which represents the standard Gutzwiller contributions from all the periodic orbits which are trapped inside the unit cell [19]. In order to obtain a semiclassical approximation for  $\text{Tr} (\Gamma S)^m$ , we first use (13) at  $x = x_s$ ,  $x' = x_{s'}$  and find

$$(\Gamma S)_{j_s, j_{s'}} = 2s e^{isqa} \sqrt{\frac{k_{j'}}{k_j}} \int_0^1 dy dy' \phi_j(y) \phi_{j'}(y') \left. \frac{\partial}{\partial x} G(xy; x_{s'} y') \right|_{x=x-s}. \quad (32)$$

The completeness of the normal modes  $\sum_{j=1}^{\infty} \phi_j(y) \phi_j(y') = \delta(y - y')$  for  $0 < y, y' < 1$  allows to express the powers of  $\Gamma S$  in coordinate space as multiple integrals over the Green function

$$\begin{aligned} \text{Tr} (\Gamma S)^m = 2^m e^{inqa} \sum_{s_1, \dots, s_m} \int_0^1 dy_1 \dots dy_m & \left[ s_1 \frac{\partial}{\partial x_1} G(x_1, y_1; x_{s_2}, y_2) \right]_{x_1=x-s_1} \\ & \times \dots \\ & \times \left[ s_m \frac{\partial}{\partial x_m} G(x_m, y_m; x_{s_1}, y_1) \right]_{x_m=x-s_m}, \end{aligned} \quad (33)$$

where the winding number  $n$  is defined as

$$-n = s_1 + \dots + s_m. \quad (34)$$

The standard semiclassical expression for the Green function

$$G(x, y; x', y') = \frac{1}{2} \sum_{\alpha} \sqrt{\frac{i}{2\pi k}} \left| \frac{\partial x_{\perp}}{\partial \varphi'} \right|_{x'_{\perp}}^{-1/2} \exp \left( ikL_{\alpha} - i \frac{\pi}{2} \mu_{\alpha} \right) \quad (35)$$

can now be inserted into (33). The sum in (35) runs over all classical trajectories  $\alpha$  leading from  $(x', y')$  to  $(x, y)$ .  $L_{\alpha}$  is the length of the path  $\alpha$  and  $\mu_{\alpha}$  contains the Maslov index of the trajectory plus twice the number of reflections from the walls of the waveguide. Due to the special geometry the Maslov index happens to be zero for all trajectories.  $\varphi$  and  $x_{\perp}$  denote the direction of the trajectory and the coordinate normal to it, respectively.

The integrals in (33) are evaluated in the saddle-point approximation. The condition of stationary phase is satisfied for all periodic orbits  $p$  of the unit cell with periodic boundary conditions, *i.e.*, whenever a periodic orbit leaves the unit cell to the left or to the right, it is

reinjecting from the opposite side.  $\text{Tr}(\Gamma S)^m$  contains all those orbits for which this happens exactly  $n_p = m$  times, irrespective of which of the two boundaries is hit. In contrast,  $n_p$  defined in (34) counts the number of reinjections including a sign according to the direction, such that  $n_p$  finally represents the number of windings of the periodic orbit around the unit cell (see Fig. 7). Obviously the orbits contributing to the total phase have a winding number  $n_p = 0$  and for the other orbits we have  $|n_p| < m_p$ . We obtain

$$\tilde{d}(E, q) = \frac{1}{2\pi\hbar} \sum_{p,r} w_{p,r} T_p \exp\left(\frac{i}{\hbar} r S_p + i r n_p q a - i \frac{\pi}{2} r \mu_p\right), \quad (36)$$

where  $r = -\infty, \dots, \infty$  (excluding  $r = 0$ ),  $p$  is summed over the primitive periodic orbits,  $w_{p,r} = |\det(M_p^r - 1)|^{-1/2}$ ,  $M = \partial(x_\perp, \varphi)/\partial(x'_\perp, \varphi')$  is the stability matrix of the periodic orbit  $p$ , and  $S_p = \hbar k L_p$  is the corresponding action. The discrete translation symmetry results in an additional phase which depends on the winding number of the orbit. Eq. (36) represents a special case of the general result obtained in [7]. According to Ref. [7], the additional phase factors are related to the characters  $\chi(n, q)$  of the irreducible representations of the group of lattice translation.

### B. Diagonal approximation for $S_N(n, \tau)$

In the following we derive the semiclassical approximation for  $S_N(n; \tau)$  in the diagonal approximation [20]. Using Eqs. (19) and (26), we have from (36)

$$\tilde{d}(x, n) = \frac{1}{2\pi\hbar\langle d_1 \rangle} \sum_{p,r} \delta_{n, r n_p}^{(N)} w_{p,r} T_p \exp\left(\frac{i}{\hbar} r S_p + i \frac{\pi}{2} r \mu_p\right).$$

Here  $\delta_{n,m}^{(N)}$  denotes a Kronecker delta with the arguments taken modulo  $N$ . Expanding the actions according to  $S_p(E \pm \epsilon/2) \simeq S_p(E) \pm T_p \epsilon/2$ , we have

$$\begin{aligned} S_N(n; \tau) &= \left\langle \int_{-\infty}^{\infty} d\xi e^{-2\pi i \xi \tau} \tilde{d}(x + \xi/2, n) \tilde{d}(x - \xi/2, n) \right\rangle \\ &= \frac{1}{(2\pi\hbar\langle d_1 \rangle)^2} \int_{-\infty}^{\infty} d\xi e^{-2\pi i \xi \tau} \left\langle \sum_{p,r} \sum_{p',r'} \delta_{n, r n_p}^{(N)} \delta_{n, r' n_{p'}}^{(N)} w_{p,r} w_{p',r'}^* T_p T_{p'} \right. \\ &\quad \left. \times \exp\left(\frac{i}{\hbar}(r S_p - r' S_{p'}) + \frac{i}{2\hbar}(r T_p + r' T_{p'})\epsilon + i \frac{\pi}{2}(r \mu_p - r' \mu_{p'})\right) \right\rangle, \end{aligned}$$

where  $\xi = N\langle d_1 \rangle\epsilon$ . Provided the actions  $S_p$  are uncorrelated, the off-diagonal terms in the double sum over primitive periodic orbits vanish upon averaging. This is certainly the case for periodic orbits with periods less than some fraction of the Heisenberg time of the unit cell,  $T_p \lesssim t_H = 2\pi\hbar\langle d_1 \rangle$ , which restricts the applicability of the present approximation to times smaller than the Heisenberg time of the unit cell, or equivalently, to  $\tau \lesssim 1/N$ . Furthermore we note that pairs of time-reversed orbits have in general opposite winding numbers. However, periodic orbits with  $n_p = 0$  or  $N/2$  give rise to an additional degeneracy, since in these cases  $-n_p = n_p \pmod{N}$ . We define the coherence factor

$$\gamma_n = \begin{cases} 2 & \text{for } n = 0, N/2, \\ 1 & \text{otherwise,} \end{cases} \quad (37)$$

and obtain

$$S_N(n; \tau) \simeq \gamma_n \tau N^2 \sum_{p,r} \delta_{n, rn_p}^{(N)} |w_{p,r}|^2 T_p \delta(rT_p - 2\pi\hbar\langle d_1 \rangle N\tau). \quad (38)$$

For  $n = 0$ , the form factor  $S_N(0; \tau)$  is just the conventional spectral form factor  $K_N(\tau)$  for the composite system, *i.e.*, for a billiard chain with periodic boundary conditions (2). The primitive periodic orbits of the entire chain have winding numbers  $n_p$  which are multiples of  $N$ , as opposed to the periodic orbits of the unit cell. The Kronecker delta in Eq. (38) ensures that for  $n = 0$ , only periodic orbits of the entire chain contribute.

The sum over periodic orbits in Eq. (38) can be evaluated as follows. According to appendix C, it can be replaced by the coarse-grained classical propagator  $P(n; t)$  defined in Eqs. (B1) and (B10). Furthermore, the classical dynamics in the periodic chain is diffusive in the  $x$ -direction (provided direct trajectories are eliminated). This is due to the chaotic scattering in the unit cells. Under these circumstances,  $P(n; t)$  is given by the expression (B5) derived in appendix C. In order to show that the classical dynamics in the billiard chain is adequately described by Eq. (B5), we have performed numerical simulations of the classical dynamics in periodic chains. The chains consist of  $N = 8$  or  $N = 128$  copies of the unit cell shown in Fig. 3. The radii of the half discs have been chosen large enough so as to eliminate direct bouncing-ball trajectories ( $R_- = 0.8$  and  $R_+ = 0.4$  in units of the channel width). The lengths of the straight-channel sections are  $\sim 0.1$  in the same units. The results of the numerical simulations are shown in Fig. 8 (solid dots), as a function of the trajectory length  $l = \hbar kt/m$ . For a given trajectory length  $l$ , we have started  $10^6$  trajectories and calculated the average probability to move  $n$  unit cells away from the starting point. For convenience, the results are given as a function of lengths  $l$  rather than times  $t$ . Also shown is a fit to Eq. (B5). The fitting parameter is the diffusion constant  $D$ . In the case shown, we obtain for the scaled diffusion constant  $D m/\hbar k a^2 \simeq 0.082$ . We observe good agreement between the numerical simulations and the results of Eq. (B5).

Replacing the sum over periodic orbits in Eq. (38) by the appropriate expression for the coarse-grained classical propagator, we obtain (neglecting repetitions of periodic orbits, since primitive periodic orbits proliferate exponentially)

$$\begin{aligned} S_N(n; \tau) &\simeq \gamma_n \tau N^2 P(n; 2\pi\hbar N\langle d_1 \rangle \tau) \\ &\simeq \gamma_n N \sqrt{\frac{N\tau}{2g_1}} \sum_{\mu} \exp\left(-\frac{\pi}{2g_1\tau} \frac{(n - \mu N)^2}{N}\right), \end{aligned} \quad (39)$$

where we have introduced the dimensionless parameter

$$g_1 = \frac{2\pi^2\hbar\langle d_1 \rangle D}{a^2}.$$

The parameter  $g_1$  is analogous to the dimensionless conductance of disordered conductors [15]. Note that it is defined with respect to the unit cell. However, since we do not assume static disorder within the unit cell, the analogy is purely formal.

Eq. (39) is the central result of this section. It relates the quantum spectral form factor  $S_N(n; \tau)$  to the classical diffusion propagator  $P(n; t)$  of winding numbers  $n$ . According to Eq. (39), the behaviour of  $S_N(n; \tau)$  depends crucially on the values of  $N$  and  $g_1$ . We distinguish two cases,  $g_1/N^2 > 1$  and  $g_1/N^2 < 1$ . The spectral properties are qualitatively different in these two regimes. For  $g_1/N^2 > 1$ , the classical dynamics becomes ergodic before the energy-time uncertainty relation allows to resolve the inter-band spacing. This corresponds to a time scale of the order of the Heisenberg time of the unit cell,  $t_H = 2\pi\hbar\langle d_1 \rangle$ , or equivalently  $\tau \sim 1/N$ . The sampling of the energy bands by discrete Bloch numbers  $q$  is then too coarse to reveal that continuous bands are underlying the discrete levels, and the full spectrum appears as a superposition of  $N$  independent spectra.

For  $g_1/N^2 < 1$ , on the other hand, we have  $g_1\tau < N$  throughout the range of validity of Eq. (39) ( $0 < \tau \lesssim 1/N$ ) and the sum in (39) can be restricted to  $\mu = 0$ . Classically this means that the diffusion cloud generated by the propagator of winding numbers is still well localized at times corresponding to the Heisenberg time of the unit cell ( $\tau \sim 1/N$ ). Semiclassically, the coarse-grained diffusion propagator encodes the quantum-mechanical spectral correlations due to the existence of energy bands. At times of the order of  $\tau \sim 1/N$ , where individual bands begin to be resolved, the spectrum appears to be  $N$ -fold degenerate. As anticipated in the introduction, the clustering of the levels into bands is reflected in the spectral form factor: at  $\tau \sim 1/N$ , the form factor exhibits a peak of the order of  $N$ ,  $S_N(0; \tau) \sim N$ . Hence, for  $g_1/N^2 < 1$ , the semiclassical expression Eq. (39) describes the effect of the quantum levels clustering into bands and relates this to the space-time dependence of the classical diffusion propagator.

In the remainder of this section, we discuss the signatures of level clustering in numerical band spectra and compare with the predictions of Eq. (39). We have calculated the quantum-mechanical form factors  $S_N(n; \tau)$  for chains with  $N = 8$  and  $N = 128$  unit cells, respectively, and with the same geometrical parameters as used in the classical simulations described above. Since  $S_N(n; \tau)$  is not self-averaging with respect to energy, we have taken the mean of seven samples with slightly different geometries (the relative deviations are of the order of a few de Broglie wavelengths). In addition, we have performed an energy average, around a mean energy of  $2mE/\hbar^2 \simeq 8.9 \times 10^3$ . For unit channel width, this corresponds to 30 open channels. Fig. 9(a) shows the quantum data for  $N = 128$  and winding numbers  $n = 0, 2, 4, 8$  (solid lines). Fig. 9(b) shows the quantum data for  $N = 8$  and winding numbers  $n = 0, 1, 2, 3$  (solid lines). In both cases, the semiclassical approximation according to Eq. (39) is also shown (dashed lines). We observe reasonable agreement with the semiclassical result for times  $\tau \lesssim 1/N$ . For larger times, the diagonal approximation leading to Eq. (39) is inappropriate as remarked above. In the present section, we restrict our discussion to times  $\tau \lesssim 1/N$ .

For  $N = 128$  as well as for  $N = 8$ , the quantum data for zero winding number ( $n = 0$ ) are enhanced by a factor of two, in keeping with the prediction of Eqs. (37) and (39). For  $n = 0$  and for very small times  $\tau \ll 1/N$ , we observe a square-root dependence of the form factor,  $S_N(0; \tau) \sim \sqrt{\tau}$ . This law persists up to  $\tau \sim 1/N$  and can be understood in terms of the behaviour of  $P(0; t)$ . For small times,  $P(0; t) \sim 1/\sqrt{t}$ . In Eq. (39) this corresponds to keeping only the  $\mu = 0$  term which leads to  $S_N(0; \tau) \sim \sqrt{\tau}$ . For very short chains, on the other hand, corrections due to the finite length modify this behaviour when the  $\mu \neq 0$  terms contribute significantly.

In both cases, the conductance is  $g_1 \simeq 33$ . In the first case ( $N = 128$ ) we have  $g_1/N^2 < 1$  and the structure of  $S_N(0; \tau)$  at  $\tau \sim 1/N$  (see Fig. 9(a)) is the signature of levels clustering into bands, as discussed above. As  $g_1/N^2$  grows larger, on the other hand, the effect of clustering of levels disappears (see Fig. 9(b), where  $N = 8$  and hence  $g_1/N^2 \simeq 1$ ). The sampling of the bands by discrete Bloch numbers is then too coarse to reveal the underlying continuous bands.

In summary we emphasize that for very small times the quantum dynamics of extended periodic quantum systems is governed by diffusion. For small  $g_1/N^2$ , the spectral form factor exhibits a peak  $\sim N$  associated with the clustering of levels into bands.

To conclude we mention a sum rule for the spectral form factors. According to appendix C, the diffusion propagator  $P(n; t)$  is normalized to  $\sum_{n=0}^{N-1} P(n; t) \simeq 1$ . Using

$$\frac{1}{N} \sum_{n=0}^{N-1} \gamma_n^{-1} S_N(n; \tau) \simeq \tau N \sum_{n=0}^{N-1} P(n; 2\pi\hbar\langle d_1 \rangle N\tau),$$

this implies a sum rule for the spectral correlators  $S_N(n; \tau)$  for  $\tau < 1/N$ . Together with (30) we have for large  $N$

$$\frac{1}{N} \sum_{n=0}^{N-1} \gamma_n^{-1} S_N(n; \tau) \simeq \begin{cases} \tau N & \text{for } \tau \lesssim 1/N \\ 1 & \text{for } \tau \gg 1. \end{cases} \quad (40)$$

This sum rule is shown in Fig. 10. Also shown is the expectation according to Eq. (40).

## V. BALLISTIC SPREADING AND THE SCALING OF THE FORM FACTOR

In sections III and IV, the behaviour of the spectral form factor  $S_N(n; \tau)$  has been determined for very large times and for small times. In the first case, for times of the order of the inverse intra-band spacing, we have  $S_N(0; \tau) \sim \gamma_n$ , corresponding to quasi-periodic motion. In the second case, for  $\tau \lesssim 1/N$ , the quantum dynamics is diffusive. In this regime, and for  $g_1/N^2 < 1$ , spectral correlations due to the clustering of levels lead to a pronounced peak in  $S_N(0; \tau)$ , at times of the order of  $\tau \sim 1/N$ . How are these two regimes to be connected? In the present section we develop a theory for the spectral form factor at intermediate times.

The derivation of Eq. (39) is based on the diagonal approximation which is known to fail for times  $\tau > 1/N$ . In the limit of large  $N$ , on the other hand, the sum over  $q$  in Eq. (28) can be replaced by an integral

$$S_N(n; \tau) \simeq \frac{1}{\Delta x} \left| \frac{L}{2\pi} \int dq \sum_{\alpha} e^{inqa - 2\pi i x_{\alpha}(q)\tau} f(x - x_{\alpha}(q)) \right|^2. \quad (41)$$

According to (19) we have  $2\pi x_{\alpha}(q)\tau \sim N\tau$  and hence the phase of the integrand is rapidly oscillating for large  $\tau$ . In this case, the integral can be evaluated in the saddle-point approximation. The condition of stationary phase reads  $2\pi x'_{\alpha}(q_j) = na/\tau$  or, in terms of the unscaled energies  $E_{\alpha}(q)$ ,

$$2\pi\langle d_1 \rangle N \left. \frac{\partial E_{\alpha}}{\partial q} \right|_{q_j} = \frac{na}{\tau}. \quad (42)$$

We emphasize that the saddle points  $q_j$  depend on the parameters  $\tau, n$  and  $N$  only through the combination  $n/N\tau$ . The resulting expression for  $S_N(n; \tau)$  is

$$S_N(n; \tau) \simeq \frac{1}{\Delta x} \left| \frac{L}{2\pi} \sum_{\alpha} \sum_{q_j} \frac{f(x - x_{\alpha}(q_j))}{\sqrt{x''_{\alpha}(q_j)\tau}} e^{iq_j a - 2\pi i x_{\alpha}(q_j)\tau} \right|^2.$$

The sum over  $\alpha$  and  $q_j$  involves many terms with uncorrelated phases. Assuming some smoothing over  $\tau$ , we can justify replacing it by

$$S_N(n; \tau) = \frac{\gamma n}{\tau} F\left(\frac{n}{N\tau}\right), \quad (43)$$

where

$$F\left(\frac{n}{N\tau}\right) \simeq \frac{a^2}{4\pi^2} \frac{N}{\Delta x} \sum_{\alpha} \sum_{q_j} \frac{f^2(x - x_{\alpha}(q_j))}{\langle d_1 \rangle E''_{\alpha}(q_j)}.$$

In writing (43), we have used the fact that the saddle points are functions of  $n/N\tau$ . For  $n = 0$ , in particular, Eq. (43) implies  $S_N(0; \tau) \sim 1/\tau$ . According to Eq. (42), this behaviour corresponds to a ballistic quantum dynamics,  $\sqrt{\langle n^2 \rangle} \sim \tau$ . This is in contrast to the diffusive spreading derived for short times,  $\langle n^2 \rangle \sim \tau$  for small  $\tau$ .

Clearly, the ballistic spreading is limited by the finite system size. We denote the time it takes for the distribution in  $n$  to spread over the entire system by  $\tau^*$ . This is a time of the order of the inverse intra-band spacing. According to the discussion in section III,  $\tau^*$  is just the time where the form factor  $S_N(n; \tau)$  saturates at its asymptotic value. This saturation, discussed above in section III B, is not described by Eq. (43).

For  $n = 0$ , Eq. (43) takes a particularly simple form. Matching (43) at  $\tau = 1/N$  with the peak derived in the diagonal approximation, we find

$$F(0) = 1/\sqrt{2g_1}. \quad (44)$$

Furthermore, since  $S_N(0; \tau^*) \simeq 2$ , we have  $\tau^* \simeq F(0)/2$ . The behaviour of  $S_N(0; \tau)$  for  $g_1/N^2 < 1$  is now completely determined on all time scales. We have

$$S_N(0; \tau) \sim 2 \begin{cases} F(0) N\sqrt{\tau N} & \text{for } 0 < \tau < 1/N \\ F(0)\tau^{-1} & \text{for } 1/N \lesssim \tau < F(0)/2 \\ 1 & \text{for } \tau > F(0)/2. \end{cases} \quad (45)$$

This prediction is tested numerically in Fig. 11.  $S_N(0; \tau)$  is shown for various values of  $N$  with otherwise unchanged parameters in (a) and for one particular value of  $N$  on a doubly logarithmic scale in (b). The dashed lines show the prediction of (45). Fig. 11(a) shows that the  $N$ -dependence of the quantum data are adequately described by Eq. (45). In Fig. 11(b), one can distinguish several time regimes, as expected from Eq. (45): First, for very short times the form factor increases according to  $\sim \sqrt{\tau}$ , as predicted by Eq. (45), which reflects the underlying classical diffusion. This behaviour continues up to  $\tau \sim 1/N$ . Second, the peak in  $S_N(0; \tau)$  at  $\tau \sim 1/N$  is a signature of the levels clustering into bands. Accordingly, the height of the peak scales as  $\sim N$ . Third, for larger times,  $S_N(0; \tau)$  decays as  $\sim 1/\tau$ . This is consistent with a ballistically spreading quantum distribution,  $\sqrt{\langle n^2 \rangle} \sim \tau$ . In this regime

the curves corresponding to different values of  $N$  coincide (see Fig. 11(a)) as predicted by Eq. (45). Fourth, the form factor saturates at  $\tau^*$ .

As  $N \rightarrow \infty$ , the spectral form factor approaches a universal function. The diffusive domain  $0 < \tau < 1/N$  shrinks and for  $\tau \leq \tau^*$  the form factor is dominated by the  $1/\tau$  behaviour which reflects the formation of continuous bands. This behaviour was not discussed before, and is one of the most important results of the present work.

We should finally note that periodic systems in  $d$  dimensions will exhibit a  $\tau^{-d}$  behaviour, as can be easily seen from the derivation above.

## VI. CONCLUSIONS

In the present article, we have investigated the implications of a discrete translation symmetry for the spectral correlations of quasi one-dimensional quantum systems with chaotic classical dynamics. The decisive new feature here, as compared to disordered systems, is the presence of discretized energy bands. We have introduced a generalized spectral form factor involving spectral correlations both for identical as well as for non-identical Bloch numbers. We have shown in detail how the time-dependence of this form factor reflects the quantum dynamics in the periodic system:

(i) For small times, the form factor was shown to be semiclassically equivalent to the coarse-grained classical propagator. In the present case, chaotic scattering implies classical diffusion in the extended system. This enabled us to derive an explicit expression for the form factor, depending only on the diffusion constant and the system size.

(ii) At  $\tau \sim 1/N$ , the spectral form factor exhibits a peak due to level clustering provided the discretization by the Bloch numbers is sufficiently fine in order to reveal the underlying smooth bands. The height of the peak corresponds to the number of strongly correlated levels and hence it is proportional to  $N$ .

(iii) For  $1/N \lesssim \tau < \tau^*$ , we have derived a universal scaling law for the form factor. This regime corresponds to ballistic quantum dynamics and is restricted by the time  $\tau^*$  needed to ballistically cover the entire system.

(iv) For  $\tau > \tau^*$ , the form factor attains its asymptotic constant value. This regime corresponds to quasi-periodic motion.

We emphasize once again that our results — tested numerically using the example of a quasi one-dimensional periodic chain of chaotic billiards — are more generally valid (see also [10]) and in fact universal. Finally we note that the transition from a periodic chain to a quasi one-dimensional disordered system is also governed by a universal law. A study concerned with the effect of introducing disorder in the present framework is under way.

## ACKNOWLEDGEMENTS

The research reported in this work was supported by grants from the US Israel Binational Science Foundation and the Minerva Center for Nonlinear Physics. Three of us (TD, BM and HS) would like to thank the the Weizmann Institute of Science, Rehovot (Israel), for the kind hospitality during several visits. BM would like to thank the Max Planck Institute for Physics of Complex Systems, Dresden (Germany), for financial support.

## APPENDIX A: THE $S$ -MATRIX OF THE UNIT CELL

In this appendix we briefly describe the numerical computation of the generalized  $S$ -matrix of the unit cell needed according to (17) for the quantization of the periodic billiard chain. As shown in Fig. 3, the unit cell consists of two half discs with radii  $R_1$  and  $R_2$ . For the method we employ here, it is essential that the projections of the half discs onto the  $x$ -axis do not overlap (see Fig. 3). This allows us to express the total  $S$ -matrix in terms of the reflection and transmission matrices of a single half disc in a waveguide using the concatenation formulae

$$\begin{aligned} t &= t_2(1 + r'_1[1 - r_2r'_1]^{-1}r_2)t_1 \\ r &= r_1 + t'_1[1 - r_2r'_1]^{-1}r_2t_1 \\ t' &= t'_1[1 - r_2r'_1]^{-1}t'_2 \\ r' &= r'_2 + t_2r'_1[1 - r_2r'_1]^{-1}t'_2. \end{aligned} \tag{A1}$$

Here  $r_1, r'_1$  and  $t_1, t'_1$  describe the scattering off the left half disc, while  $r_2, r'_2$  and  $t_2, t'_2$  describe the scattering off the right half disc. The definitions of these matrices are analogous to the definition of  $r, r'$  and  $t, t'$  in (14) and (15).

The computation of the  $S$ -matrix of a single half disc inside the waveguide remains to be explained. We assume that its center is located at the origin. Other reference points as well as the reflection from  $y = 1/2$  (which is needed to obtain the right obstacle in Fig. 3) can be obtained in terms of unitary transformations. Moreover we use the reflection symmetry of the half disc in order to decompose the  $S$ -matrix into a symmetric part  $S^+$  and an antisymmetric part  $S^-$ , which are related to the reflection and transmission matrices according to  $S^\pm = t \pm r$ . The calculation of  $S^-$  including evanescent modes has been described in detail in [13] and  $S^+$  can be found by straightforward analogy. The result can be summarized in the matrix equation

$$S^\pm = 1 + C^\pm T (P^\pm)^{-1} (C^\pm)^{\text{tr}}. \tag{A2}$$

Here  $T$  denotes the transition matrix for the scattering from a circle in the free plane which is diagonal in angular momentum representation and has the elements  $T_l(kR) = -J_l(kR)/H_l^+(kR)$ . The matrix

$$P_{ll'}^\pm = \delta_{ll'} - [F_{l-\nu}(2k) \mp F_{l+\nu}(2k)]T_\nu(kR) \tag{A3}$$

with

$$F_l(x) = 2 \sum_{n=1}^{\infty} \cos\left(\frac{l\pi}{2}\right) H_l^+(nx) \tag{A4}$$

describes the coupling of angular momenta due to the presence of the waveguide. The angular momentum runs over all positive even numbers for  $S^-$  and over all positive odd numbers for  $S^+$ . For the numerical computation of the only conditionally convergent series (A4), a method has been developed in [22]. Finally, the matrix

$$C_{j,l}^\pm = i\sqrt{\frac{2}{k_j}}(R_{j,l} \pm R_{j,-l}) \tag{A5}$$



with

$$R_{j,l} = \left( \frac{-i \operatorname{sgn}(l) k_j + j\pi}{k} \right)^{|l|} \quad (\text{A6})$$

contains the expansion coefficients of the normal mode  $n$  in the free-channel region in the angular-momentum basis which is appropriate close to the semicircular obstacles. The method described in this appendix has been successfully applied to compute  $S^-$  up to values of  $k \approx 1000$  [19], which is far beyond what is needed within the present application.

## APPENDIX B: CLASSICAL MECHANICS OF PERIODIC CHAINS

In this appendix, we discuss the classical mechanics of a periodic chain of chaotic scattering elements with periodic boundary conditions. We assume that the chain extends along the  $x$ -direction and consists of  $N$  identical copies of a unit cell (of length  $a$ ). Let  $\mathbf{z} = (x, y, \varphi)$  denote a phase space vector on the energy shell ( $y$  and  $\varphi$  are the transversal coordinate and the direction of the momentum, respectively). The dynamics on the energy shell is governed by the propagator

$$P(\mathbf{z}, \mathbf{z}'; t) = \delta(\mathbf{Z}(\mathbf{z}', t) - \mathbf{z}), \quad (\text{B1})$$

where  $\mathbf{Z}(\mathbf{z}', t)$  denotes the trajectory started at  $t = 0$  from  $\mathbf{z}'$ . Since the unit cell is chaotic (neglecting the possible influence of an infinite horizon), both  $y$  and  $\varphi$  are effectively decorrelated on time scales larger than the ergodic time of the unit cell. Consequently, we obtain diffusive spreading in the  $x$ -direction

$$\langle x^2 \rangle \simeq Dt.$$

The classical propagator solves the diffusion equation

$$\left[ \frac{\partial}{\partial t} - \frac{D}{2} \frac{\partial^2}{\partial x^2} \right] P(x, x'; t) = 0, \quad (\text{B2})$$

with the boundary condition  $P(x; 0) = \delta^{(L)}(x)$ , where  $\delta^{(L)}(x)$  is the  $L$ -periodic delta function. The propagator is normalized according to  $\int_0^L dx P(x; t) = 1$ . The solution of (B2) can be easily found by representing  $P(x, t)$  in terms of eigenfunctions of the stationary problem. We obtain

$$P(x; t) = \frac{1}{L} \sum_{\nu=-\infty}^{\infty} \exp \left[ 2\pi i \nu \frac{x}{L} - D \left( \frac{2\pi \nu}{L} \right)^2 \frac{t}{2} \right]. \quad (\text{B3})$$

It is appropriate to introduce an additional coarse graining of the coordinate  $x$  by defining

$$n = [x/a] \quad (\text{B4})$$

where  $[..]$  denotes the integer part. As will be seen below,  $n$  can be interpreted as the winding number of a trajectory around the unit cell (with periodic boundary conditions). From Eq. (B3) we have

$$P(n; t) \simeq \frac{1}{N} \sum_{\nu=-\infty}^{\infty} \exp \left( 2\pi i \nu \frac{n}{N} - \frac{D}{a^2} \left[ \frac{2\pi \nu}{N} \right]^2 \frac{t}{2} \right), \quad (\text{B5})$$

which after Poisson summation can be written as

$$P(n; t) = \frac{a}{\sqrt{2\pi Dt}} \sum_{\mu=-\infty}^{\infty} \exp \left( -\frac{a^2}{2Dt} [n - \mu N]^2 \right). \quad (\text{B6})$$

Due to the finite system size, the propagator  $P(n; t)$  exhibits a crossover from diffusion to equidistribution on the time scale of the Thouless time  $t_D = L^2/\pi D$ . Indeed for small times  $t \rightarrow 0$ , only the  $\mu = 0$  term contributes in (B6) and we have

$$P(n; t) \simeq \frac{a}{\sqrt{2\pi Dt}} \exp\left(-\frac{n^2 a^2}{2Dt}\right). \quad (\text{B7})$$

For large times ( $t \gg t_D$ ) the dominant term in (B3) is  $\nu = 0$  and  $P(n; t)$  saturates at

$$P(n; t) \simeq \frac{1}{N}. \quad (\text{B8})$$

This behaviour is summarized in Figs. 12 and 13. Fig. 12 shows the diffusion of winding numbers. The solid dots are a numerical simulation for an infinite periodic chain. The solid line is a fit to the diffusion law  $\langle x^2 \rangle = Dt$ , or equivalently  $\langle n^2 \rangle = Dm/\hbar ka^2 l$ . We obtain  $Dm/\hbar ka^2 \simeq 0.082$ . Fig. 13 shows  $P(n; t)$  as a function of  $n$  for three cases: (a) for  $t \ll t_D$ , (b) for  $t \simeq t_D$  and (c) for  $t > t_D$ .

So far we have derived a diffusion equation for the coarse-grained propagator  $P(n; t)$  by neglecting all details of the chaotic dynamics within the unit cell. In the following we derive an alternative expression for  $P(n; t)$  in terms of all periodic orbits of the unit cell, which will later allow to make contact with the semiclassical spectral density. For this purpose we employ (B1) and (B4) to write the coarse-grained propagator as

$$P(n; t) = \frac{1}{\Omega_1(E)} \int_{\Omega_1(E)} d\mathbf{z} d\mathbf{z}' P(\mathbf{z} + n\mathbf{a}, \mathbf{z}'; t), \quad (\text{B9})$$

where  $\mathbf{a} = (a, y = 0, \varphi = 0)$  and  $\Omega_1(E)$  denotes the volume of the energy shell for motion within the unit cell (as opposed to the volume of the energy shell for the entire chain). Since the dynamics within the unit cell is chaotic, the transition probability is effectively independent of  $\mathbf{z}'$ , and we use this to replace  $\mathbf{z}'$  by  $\mathbf{z}$ :

$$\begin{aligned} P(n; t) &\simeq \frac{1}{\Omega_1(E)} \int_{\Omega_1(E)} d\mathbf{z} d\mathbf{z}' P(\mathbf{z} + n\mathbf{a}, \mathbf{z}; t) \\ &= \int_{\Omega_1(E)} d\mathbf{z} P(\mathbf{z} + n\mathbf{a}, \mathbf{z}; t). \end{aligned} \quad (\text{B10})$$

We have now expressed the coarse-grained propagator by the probability to return to the same phase-space point up to a translation by  $n$  lattice vectors or, when interpreted in the unit cell, as the joint probability to return and to have completed  $n$  windings around the cylinder. The total probability to return on a compact phase space can be expressed as a sum over all periodic orbits [15] and an analogous relation for  $P(n; t)$  can be obtained in terms of the periodic orbits of the unit cell with winding number  $n$  (disregarding bouncing ball orbits). We insert (B1) into (B10) and use a linear approximation for  $\mathbf{Z}(\mathbf{z}, t)$  in the vicinity of each periodic orbit  $p$ .  $x$  and  $y$  are replaced by local coordinates  $x_\perp$  and  $x_\parallel$  aligned with the orbit, where the latter is cyclic with the length  $L_p$  of the orbit  $x_\parallel + L_p \equiv x_\parallel$ . Finally we have

$$\begin{aligned} P(n; t) &\simeq \sum_{p,r} \int_{\Omega_1(E)} dx_\parallel dx_\perp d\varphi \delta_{n, rn_p}^{(N)} \delta^{(L_p)}(L_p + 2k[t - rT_p]) \\ &\quad \times \delta\left(\frac{\partial x_\perp(t)}{\partial x_\perp(0)} \Delta x_\perp + \frac{\partial x_\perp(t)}{\partial \varphi(0)} \Delta \varphi - \Delta x_\perp\right) \delta\left(\frac{\partial \varphi(t)}{\partial x_\perp(0)} \Delta x_\perp + \frac{\partial \varphi(t)}{\partial \varphi(0)} \Delta \varphi - \Delta \varphi\right) \\ &= \sum_{p,r} \delta_{n, rn_p}^{(N)} \frac{T_p}{|\det(M_p^r - 1)|} \delta(t - rT_p), \end{aligned} \quad (\text{B11})$$

where  $T_p$  denotes the period of the periodic orbit and  $M_p$  is the monodromy matrix. The sum over  $r$  is a sum over repetitions of primitive periodic orbits  $p$ . In this way we have expressed the coarse-grained classical propagator of the extended billiard  $P(n, t)$  using periodic orbits of the unit cell. We make use of this result in the semiclassical analysis of the billiard in section IV.

## REFERENCES

- [1] M. V. Berry. Semiclassical theory of spectral rigidity. *Proc. R. Soc. Lond. A*, 400:229–251, 1985.
- [2] J. H. Hannay and A. M. Ozorio de Almeida. Periodic orbits and a correlation function for the semiclassical density of states. *J. Phys. A*, 17:3429–3440, 1984.
- [3] T. Dittrich and U. Smilansky. In *Quantum Chaos*. Cambridge University Press, Cambridge, 1995.
- [4] N. Argaman, Y. Imry, and U. Smilansky. *Phys. Rev. B*, 47:4440, 1993.
- [5] E. Doron, U. Smilansky, and T. Dittrich. The domino billiard. *Physica B*, 179:1–5, 1992.
- [6] A. G. Aronov, V. E. Kravtsov, and I. V. Lerner. Spectral correlations in disordered electronic systems: crossover from metal to insulator regime. *Phys. Rev. Lett.*, 74:1174–1177, 1995.
- [7] J. M. Robbins. Discrete symmetries in periodic-orbit theory. *Phys. Rev. A*, 40:2128, 1989.
- [8] P. Leboeuf and A. Mouchet. Tunneling and the band structure of chaotic systems. *Phys. Rev. Lett.*, 73:1360–1363, 1994.
- [9] G. Casati, B. V. Chirikov, F. M. Izrailev, and J. Ford. In G. Casati and J. Ford, editors, *Stochastic Behavior in Classical and Quantum Hamiltonian Systems*, volume 93 of *Lecture Notes in Physics*, page 334, Berlin, 1983. Springer.
- [10] T. Dittrich, B. Mehlige, H. Schanz, and U. Smilansky. unpublished.
- [11] E. Doron and U. Smilansky. Semiclassical quantization of chaotic billiards: A scattering theory approach. *Nonlinearity*, 5:1055–1084, 1992.
- [12] M. Cahay, M. McLennan, and S. Datta. Conductance of an array of elastic scatterers: A scattering-matrix approach. *Phys. Rev. B*, 37:10 125–10 136, 1988.
- [13] H. Schanz and U. Smilansky. Quantization of Sinai’s billiard – A scattering approach. *Chaos, Solitons & Fractals*, 5:1289–1309, 1995.
- [14] O. Bohigas. In M. J. Giannoni, A. Voros, and J. Zinn-Justin, editors, *Chaos and Quantum Physics*, Les Houches Summer School Sessions LII, Amsterdam, 1991. North-Holland.
- [15] T. Dittrich. Spectral statistics for 1-D disordered systems: A semiclassical approach. *Phys. Rep.*, 271:267–353, 1996.
- [16] This convention differs from that used in T. Dittrich, B. Mehlige, H. Schanz, and U. Smilansky, Ref. [10].
- [17] M. Sh. Birman and D. R. Yafaev. The spectral shift function. The work of M. G. Krein and its further development. *St. Petersburg Math. J.*, 4:833–870, 1993.
- [18] H. P. Baltes and E. R. Hilf. *Spectra of Finite Systems*. Bibliographisches Institut, Mannheim, 1976.
- [19] H. Primack, H. Schanz, U. Smilansky, and I. Ussishkin. Penumbra diffraction in the quantization of concave billiards. *J. Phys. A*, 1996. Submitted for publication.
- [20] M. Berry. Some quantum-to-classical asymptotics. In M. J. Giannoni, A. Voros, and J. Zinn-Justin, editors, *Chaos and Quantum Physics*, Les Houches Summer School Sessions LII, Amsterdam, 1991. North-Holland.
- [21] T. Dittrich, E. Doron, and U. Smilansky. *J. Phys. A*, 27:79, 1994.
- [22] R. Blümel and U. Smilansky. A simple model for chaotic scattering – II. quantum mechanical theory. *Physica D*, 36:111–136, 1989.

FIGURES

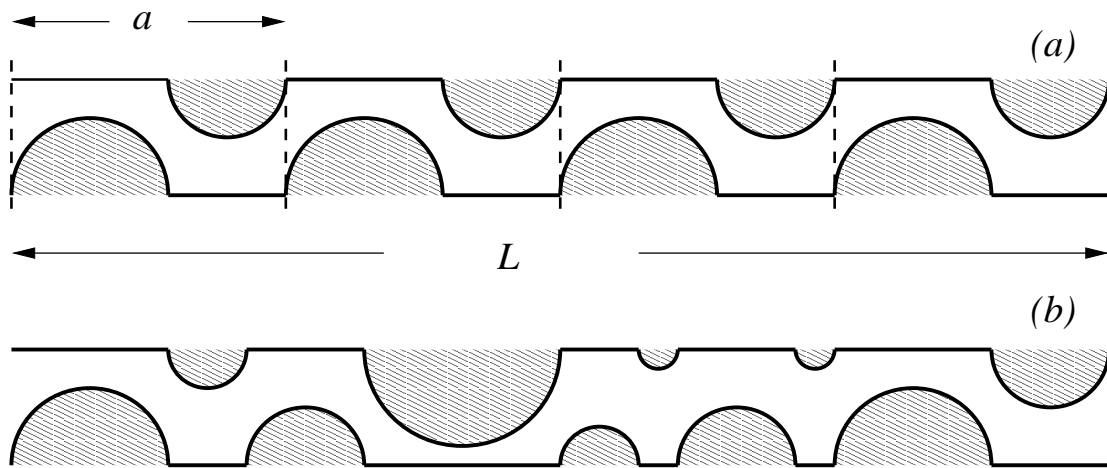


FIG. 1. Quasi one-dimensional chains of coupled billiards. (a) shows a periodic chain while (b) shows a disordered chain. In both cases periodic boundary conditions are imposed at the ends of the chains.

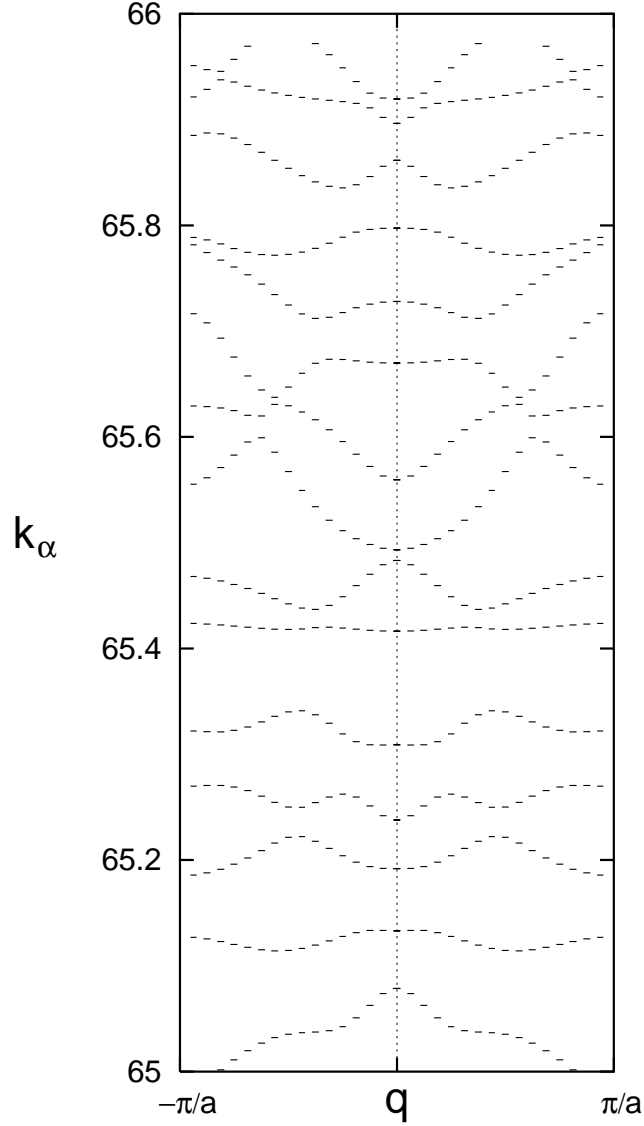


FIG. 2. Typical band spectrum of a periodic billiard chain with  $N = 32$  unit cells. Shown are the levels  $k_\alpha(q)$  as a function of the Bloch number  $q$  in the first Brillouin zone,  $-\pi/a \leq q < \pi/a$ .

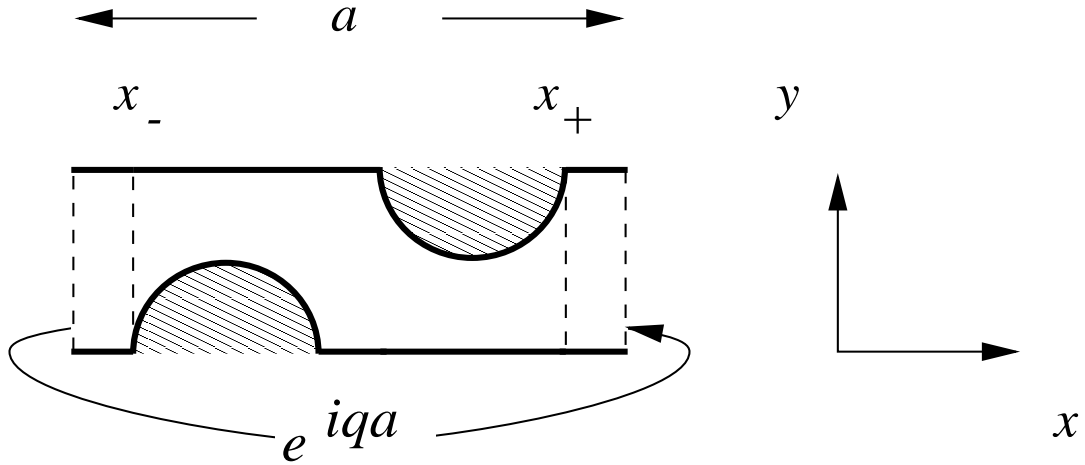


FIG. 3. Unit cell of the periodic chain of chaotic billiards. The unit cell has unit width and a length  $a$ . According to Bloch's theorem, the periodic chain can be quantized using Eq. (17). This corresponds to quantizing a single unit cell with periodic boundary conditions and an additional phase  $\exp(iqa)$ .

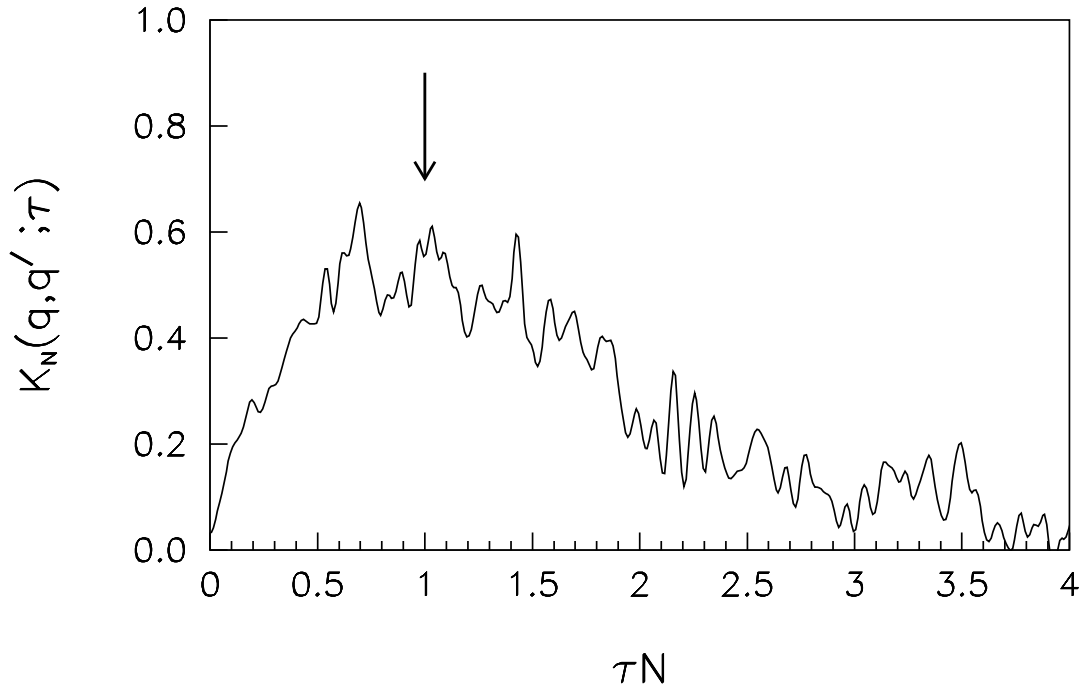


FIG. 4. Spectral form factor  $K_N(q, q'; \tau)$  for  $q \neq q'$  as a function of  $\tau N$ . For large times  $\tau > 1/N$ ,  $K_N(q, q'; \tau)$  tends to zero since levels of the same band decorrelate for  $q \neq q'$ . The arrow indicates  $\tau \sim 1/N$ , a time of the order of the inverse inter-band spacing. The data are taken from a chain with  $N = 128$  unit cells.



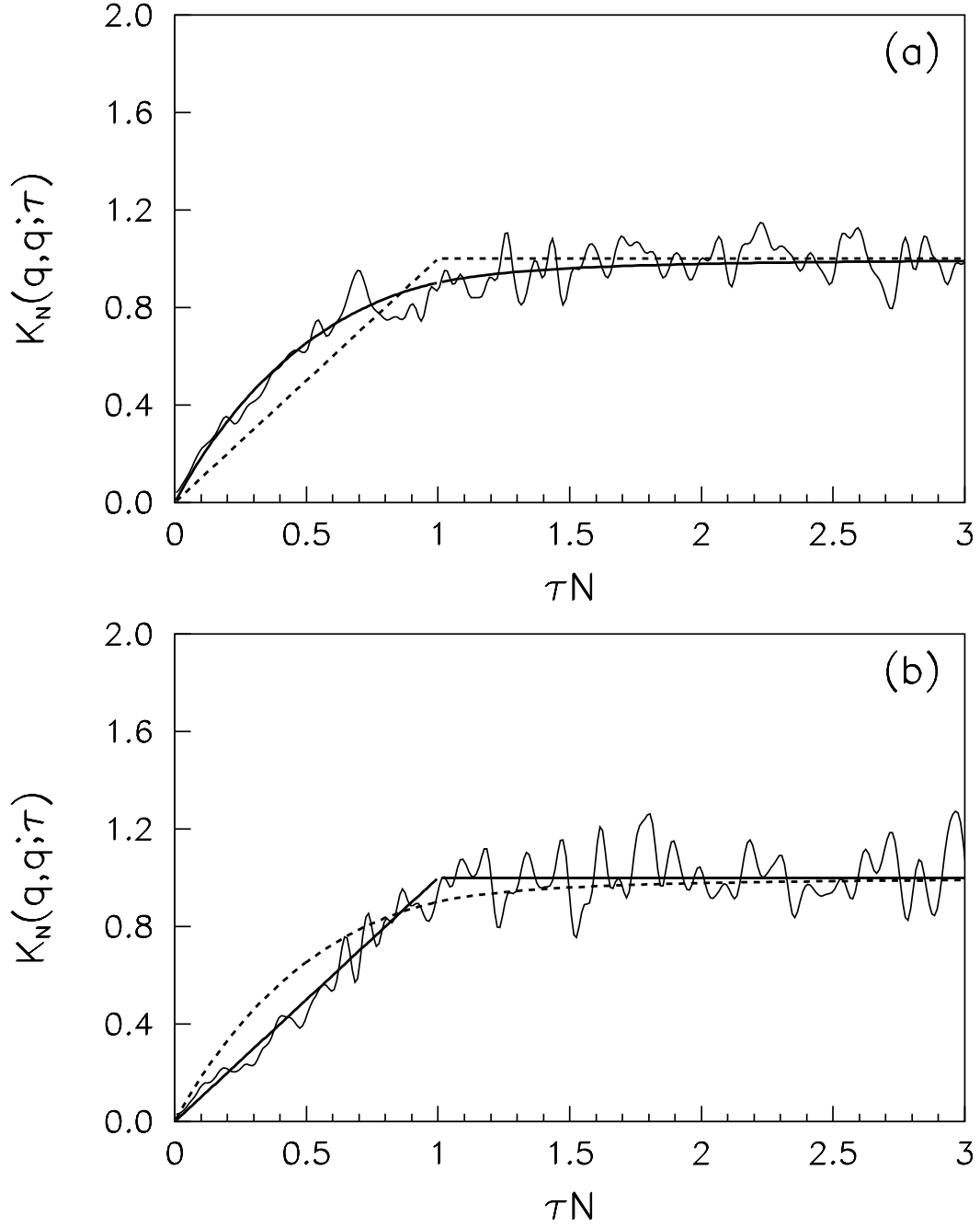


FIG. 5. Form factors  $K_N(q, q; \tau)$  for different values of the Bloch number  $q$  as a function of  $\tau N$ . In (a) we show the case  $q = 0$  where the spectrum shows GOE statistics, and in (b) the case  $q = \pi/2a$  where the spectrum shows GUE statistics.

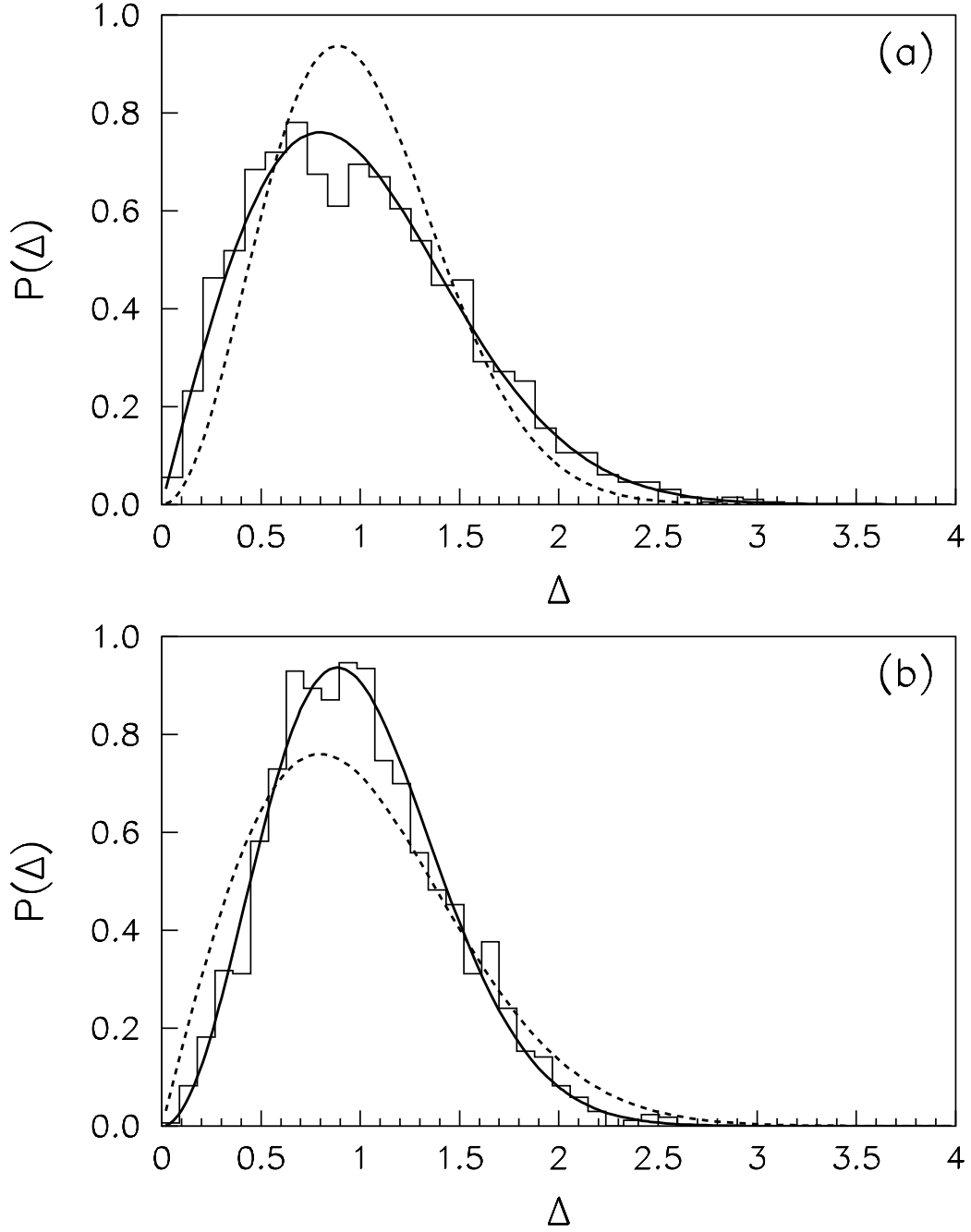


FIG. 6. Histograms  $P(\Delta)$  of the nearest-neighbour spacings  $\Delta$ , for fixed Bloch number  $q$ . (a) shows the case  $q = 0$  where the spectrum shows GOE statistics, while (b) shows the case  $q = \pi/2a$ , where the spectrum shows GUE statistics.

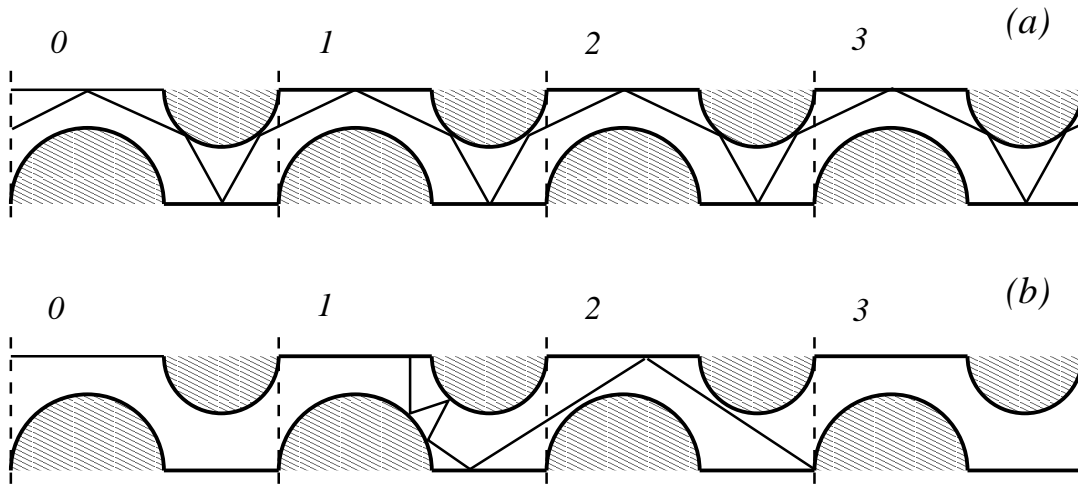


FIG. 7. Topology of periodic orbits in the periodic chain. (a) shows a periodic orbit with winding number  $n = 1$  while (b) shows a periodic orbit with winding number  $n = 0$ . Note that the periodic orbit in (b) is self-retracing.

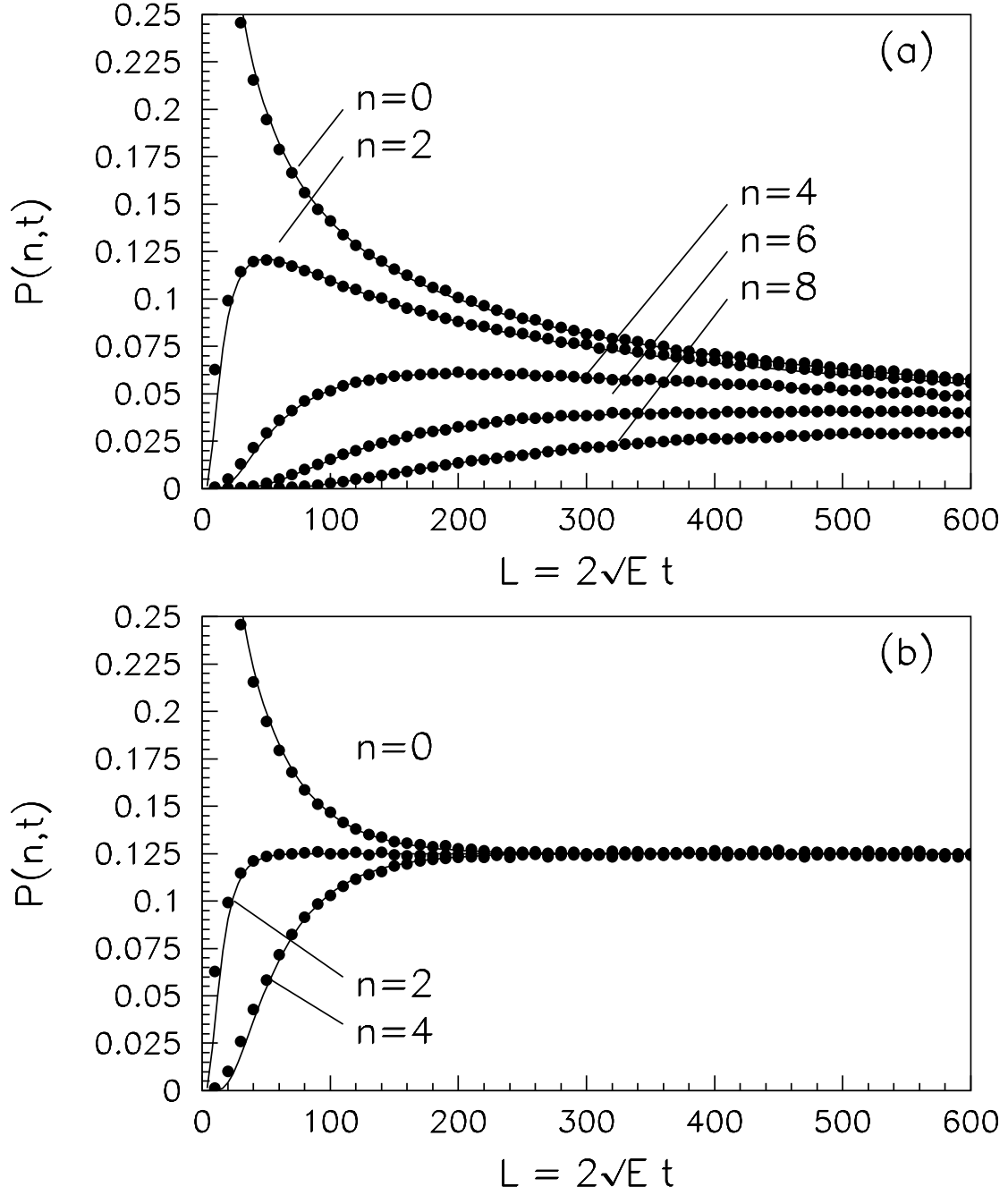


FIG. 8. Diffusion propagator  $P(n;t)$  for a periodic chain. (a) shows the distribution of  $P(n;t)$  for  $N = 128$ , (b) shows  $P(n;t)$  for  $N = 8$ , as a function of  $l = \hbar kt/m$  (the energy dependence of the classical mechanics has been scaled out). Note that for large  $t$ ,  $P(n;t)$  approaches  $1/N$  (compare Eq. (B8)).

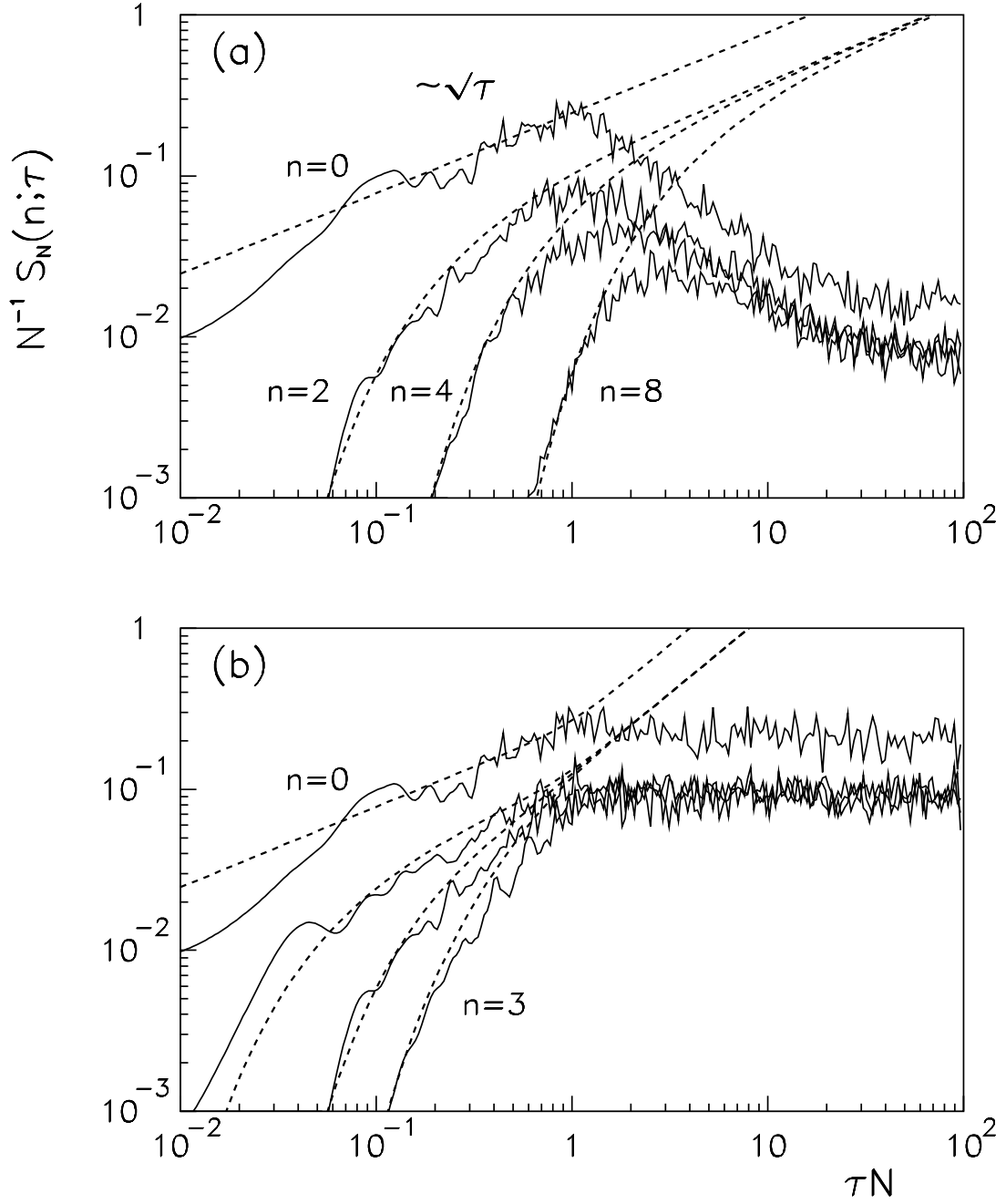


FIG. 9. Shows  $S_N(n; \tau)$  as extracted from the quantum spectrum for a periodic chain, (a) for  $N = 128$  and  $n = 0, 2, 4, 8$  and (b) for  $N = 8$  and  $n = 0, 1, 2, 3$  (solid lines). Also shown (dashed lines) are the results of the semiclassical approximation Eq. (39).

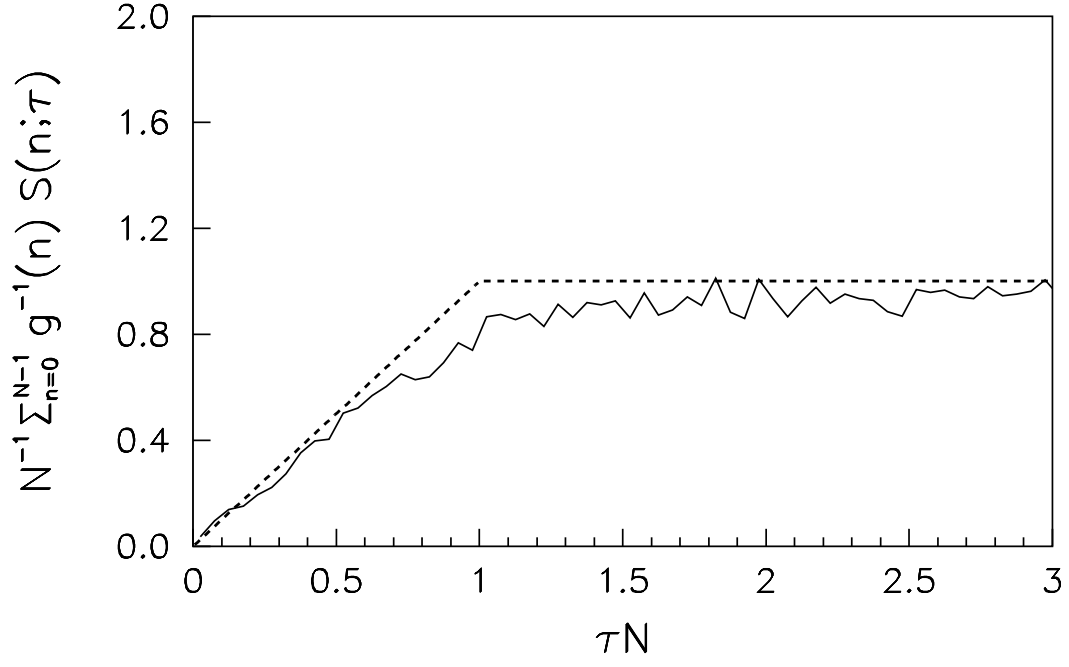


FIG. 10. Semiclassical sum rule. The solid line is the sum of the spectral form factors  $S_N(n; \tau)$ , while the dashed line is the semiclassical prediction according to Eq. (40).

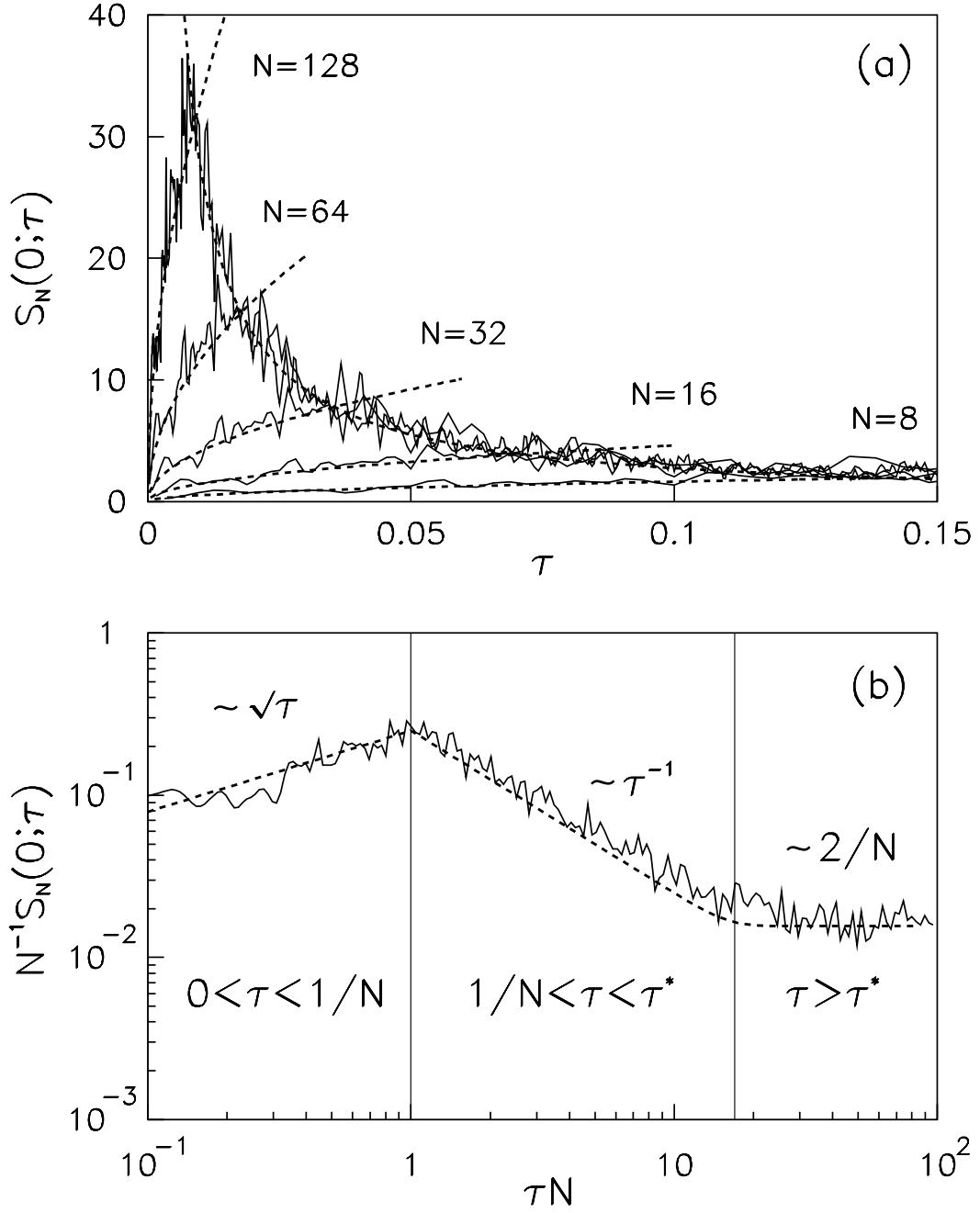


FIG. 11. Scaling of  $S_N(n; \tau)$ . (a) shows the scaling of  $S_N(n; \tau)$  with  $N$ , for  $N = 8, 16, 32, 64$  and  $N = 128$ . (b) shows the various regimes in a doubly logarithmic plot: (i) the diffusive increase  $\sim \sqrt{\tau}$  for small times, (ii) the peak  $\sim N$  at  $\tau = 1/N$  due to the level clustering, (iii) the  $1/\tau$  decay associated with ballistic quantum spreading and finally (iv) the constant asymptote at the time scale corresponding to the mean intra-band spacing due to quasi-periodic motion.

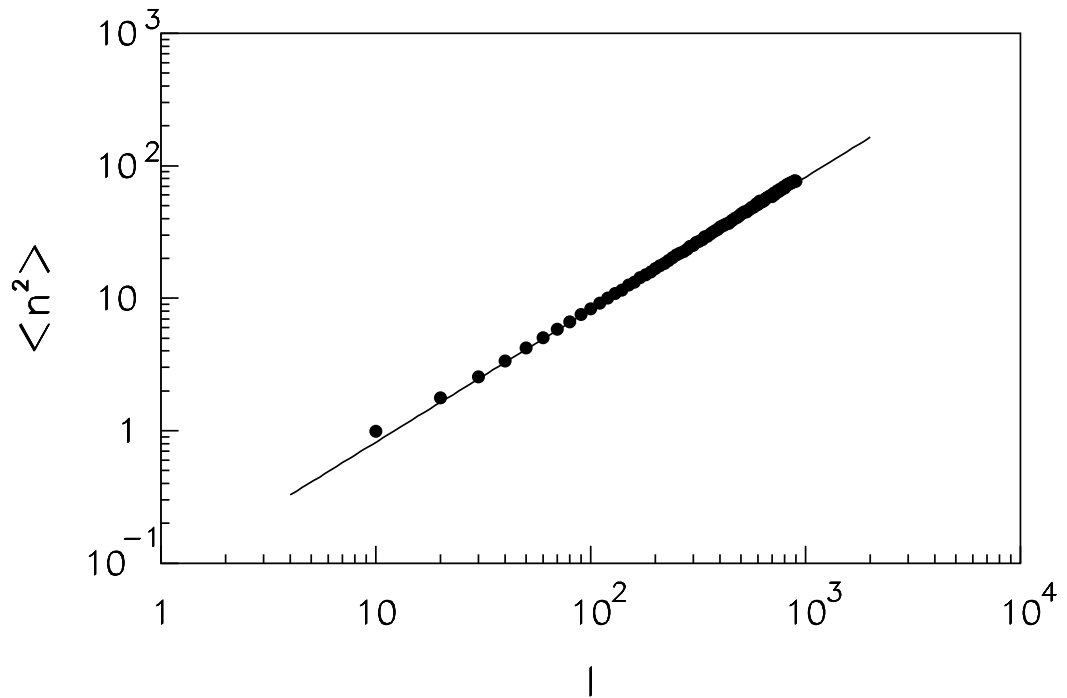


FIG. 12. Diffusion in the periodic chain. Shown is the the result of a classical simulation: The variance  $\langle n^2 \rangle$  of winding numbers  $n$  for trajectory segments of length  $l$  increases according to  $\langle n^2 \rangle \sim l$ .



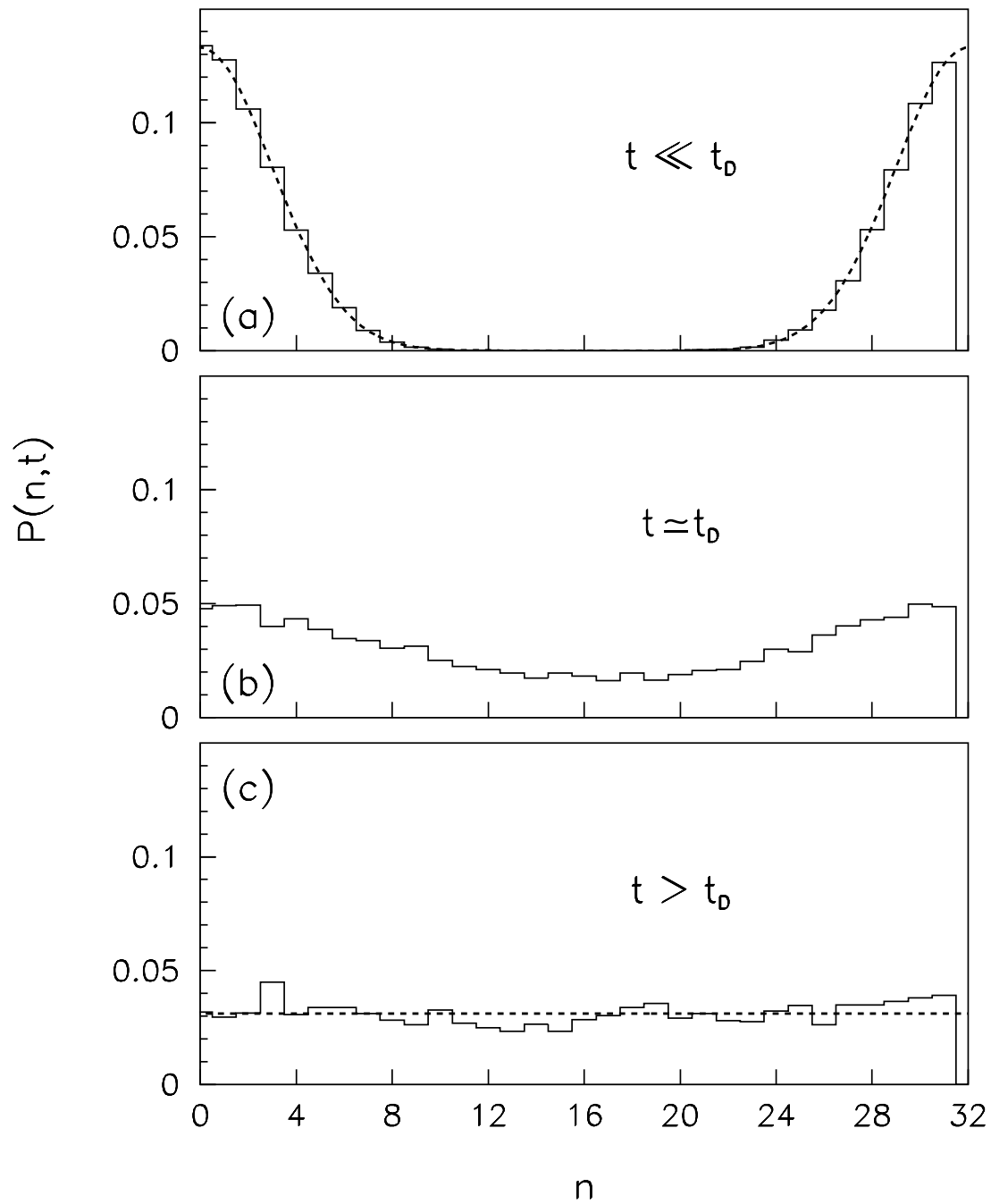


FIG. 13. The distribution of  $P(n; t)$  for three cases: (a) for  $t \ll t_D$ , (b) for  $t \simeq t_D$  and (c) for  $t > t_D$ . The dashed lines show the limiting distributions (B7) and (B8), for small and large times, respectively.